Eudragit S100-Coated PLGA Nanoparticles for Colon-Targeted Prednisolone Delivery in Ulcerative Colitis: Formulation Optimization and In Vitro Evaluation

Abhay Yadav[1], Ved Prakash Tiwari[2], Monu Kumar Kashyap[3],
Ashish Srivastava[4], Pramod Kumar Mishra[5], Karuna S Shukla[6]
[1,2,3,4,5,6]*Goel Institute of Pharmaceutical Sciences, Lucknow, U. P. India*

Abstract— **Ulcerative colitis is a relapsing inflammatory disease of the colon in which local corticosteroid exposure is desirable, whereas unnecessary systemic exposure can increase adverse effects. Prednisolone is an effective glucocorticoid; however, conventional oral delivery may release drug before the formulation reaches the distal intestine. The present work developed pH-responsive colon-targeted prednisolone nanoparticles using a biodegradable PLGA core, PVA as stabilizer and Eudragit S100 as an enteric coating polymer. Prednisolone-loaded nanoparticles were prepared by solvent displacement and optimized using a three-factor Box-Behnken design. The effects of PLGA amount, PVA concentration and Eudragit S100 amount were assessed on particle size, PDI, zeta potential, entrapment efficiency, percentage yield and 24 h cumulative release. The optimized coated nanoparticles contained PLGA 120 mg, PVA 0.6% w/v and Eudragit S100 75 mg and showed particle size of 214.6 ± 6.8 nm, PDI of 0.214 ± 0.018, zeta potential of -31.8 ± 1.6 mV, entrapment efficiency of 82.4 ± 2.1%, drug content of 96.8 ± 2.7% and 24 h release of 76.9 ± 3.1%. Sequential pH release demonstrated restricted acidic release followed by progressive drug liberation at intestinal/colonic pH. Release kinetics were most consistent with Higuchi and Korsmeyer-Peppas models, supporting diffusion-dominant release with polymer relaxation contribution. Mucin binding reached 79.4 ± 3.8% at 60 min, hemolysis remained below 5% up to 400 ug/mL and Caco-2 viability remained above 75% up to 200 ug/mL. These findings support Eudragit S100-coated PLGA nanoparticles as a promising in vitro platform for colon-targeted prednisolone delivery.**

Index Terms— **prednisolone; ulcerative colitis; colon-targeted drug delivery; PLGA nanoparticles; Eudragit S100; Box-Behnken design; pH-responsive release; mucin binding**

Highlights

- Prednisolone-loaded PLGA nanoparticles were coated with pH-responsive Eudragit S100 for colon-directed release.
- A three-factor Box-Behnken design balanced particle size, PDI, surface charge, entrapment, yield and 24 h release.
- The optimized formulation showed nanoscale size, high entrapment and reduced acidic release.
- Gray-pattern, no-grid figures with SD/error bars have been incorporated for journal-ready visual presentation.
- Mucin binding, hemocompatibility, Caco-2 viability and stability results support further preclinical evaluation.

Graphical abstract statement

Prednisolone and PLGA are co-precipitated into nanoparticles by solvent displacement, stabilized with PVA, coated with Eudragit S100 and subsequently exposed to sequential gastrointestinal pH conditions. The coating restricts acidic release and allows sustained release at higher pH, thereby supporting colon-directed corticosteroid delivery.

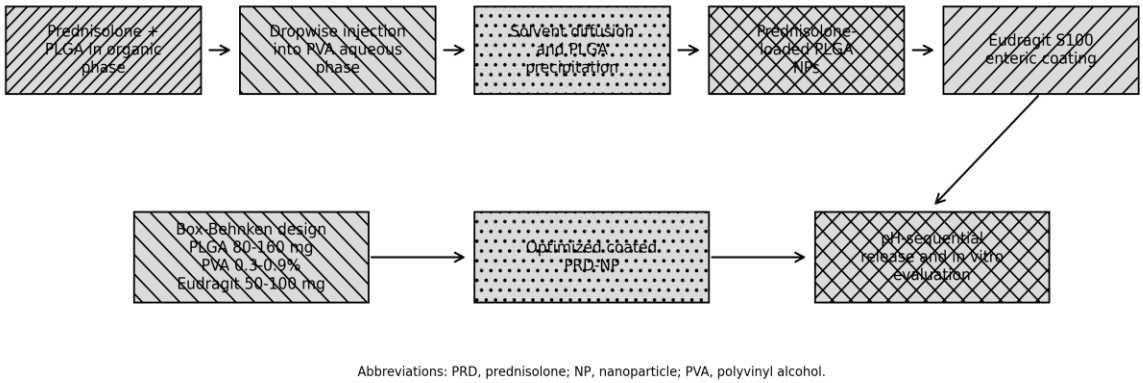

Figure 1. Formulation-development workflow and proposed pH-responsive release concept for Eudragit S100-coated prednisolone-loaded PLGA nanoparticles.

I. INTRODUCTION

Ulcerative colitis is a chronic inflammatory bowel disease characterized by continuous mucosal inflammation that typically begins in the rectum and may extend proximally through the colon. The disease involves epithelial barrier disruption, mucosal immune activation, cytokine release, oxidative stress and repeated cycles of tissue injury and repair [1-5]. Because the inflamed region is localized primarily in the large intestine, delivery systems that increase drug residence and drug availability in the colon are pharmacologically attractive.

Corticosteroids remain useful for controlling moderate-to-severe inflammatory episodes, but conventional systemic exposure may produce metabolic, endocrine, musculoskeletal, gastric and immunological adverse effects [5,6]. Prednisolone is a potent glucocorticoid that suppresses inflammatory gene expression, leukocyte recruitment, prostaglandin synthesis and cytokine release. For ulcerative colitis, the therapeutic objective is not simply systemic absorption, but adequate local anti-inflammatory exposure at the diseased colonic mucosa.

Colon-targeted drug delivery systems exploit physiological triggers such as gastrointestinal pH, transit time, microbiota-associated degradation or disease-linked mucosal changes [7-10]. pH-responsive methacrylate polymers are widely used in this context because they can protect the drug in the acidic stomach and dissolve more readily at higher intestinal pH [8,9]. Eudragit S100 is particularly relevant for delayed release because it remains relatively unionized at low pH and dissolves under more alkaline conditions.

Nanoparticulate carriers add further benefits for inflammatory bowel disease therapy, including high surface area, mucoadhesive or mucus-interactive behavior, controlled drug diffusion and potential retention at inflamed mucosa [11-13]. PLGA is a biodegradable polymer frequently used for controlled release, while PVA provides steric stabilization during solvent displacement [14-19]. The present study therefore formulated prednisolone-loaded PLGA nanoparticles, coated them with Eudragit S100 and optimized the composition using response surface methodology.

II. MATERIALS AND METHODS

2.1 Materials

Prednisolone was used as the model corticosteroid. PLGA 50:50 was selected as the biodegradable matrix-forming polymer. Polyvinyl alcohol (PVA) was used as stabilizer and Eudragit S100 as the pH-responsive enteric coating polymer. Acetone: ethanol was used as the organic solvent system. Phosphate buffer salts, hydrochloric acid, sodium hydroxide, dialysis membrane, mucin, methanol, acetonitrile and HPLC-grade water were used for analysis and in vitro evaluation.

2.2 Analytical method and stock solutions

Prednisolone stock solution was prepared by dissolving 10 mg prednisolone in 10 mL methanol to obtain 1000 ug/mL. Working standards of 5, 10, 20, 40, 60, 80 and 100 ug/mL were prepared by dilution with methanol: water 70:30. The analytical response was recorded at 247 nm. PVA aqueous solutions at 0.3, 0.6 and 0.9% w/v were prepared by heating with continuous stirring at 70°C until clear, followed by cooling to room temperature.

2.3 Preparation of prednisolone-loaded PLGA nanoparticles

Prednisolone-loaded nanoparticles were prepared by solvent displacement. Prednisolone (20 mg) and PLGA at the design-specified amount (80, 120 or 160 mg) were dissolved in 10 mL acetone: ethanol 8:2 v/v. The organic phase was injected dropwise through a 24 G needle into 40 mL aqueous PVA solution under magnetic stirring at 1000 rpm. The dispersion was stirred for 4 h at room temperature to allow organic solvent evaporation.

2.4 Eudragit S100 coating and lyophilization

For enteric coating, Eudragit S100 (50, 75 or 100 mg) was dissolved in 8 mL ethanol containing triethyl citrate (0.2 mL) as plasticizer. The coating solution was added slowly to the nanoparticle dispersion at 700 rpm and stirred for 2 h. The pH was maintained at 6.8 using 0.1 N NaOH to prevent abrupt polymer precipitation. The coated dispersion was centrifuged at 15000 rpm for 30 min at 4°C, washed twice with distilled water and lyophilized using 5% w/v mannitol as cryoprotectant.

2.5 Box-Behnken experimental design

A three-factor, three-level Box-Behnken design was used to evaluate the effects of PLGA amount (X1), PVA concentration (X2) and Eudragit S100 amount (X3) on particle size, PDI, zeta potential, entrapment efficiency, process yield and 24 h cumulative release. The independent variables and levels are presented in Table 1. Selection of the optimized batch was based on simultaneous desirability rather than a single response.

Table 1. Independent variables and levels used in the Box-Behnken design.

Independent variable	Low (-1)	Middle (0)	High (+1)
X1: PLGA amount (mg)	80	120	160
X2: PVA concentration (% w/v)	0.3	0.6	0.9
X3: Eudragit S100 amount (mg)	50	75	100

2.6 Particle size, PDI and zeta potential

Particle size and PDI were determined by dynamic light scattering after suitable dilution with filtered distilled water. Zeta potential was measured after dilution in an appropriate aqueous medium. These measurements were used to evaluate nanoscale formation, size distribution and electrostatic stability.

2.7 Drug content, entrapment efficiency and process yield

Nanoparticles equivalent to 10 mg formulation were dissolved in 5 mL acetonitrile, vortexed for 5 min and diluted to 10 mL with methanol: water 70:30. The solution was centrifuged at 10000 rpm for 10 min, and the supernatant was analyzed at 247 nm. Entrapment efficiency was calculated as actual drug entrapped divided by total drug added, multiplied by 100. Percentage yield was calculated from recovered dried nanoparticles relative to theoretical solid content.

2.8 pH-sequential in vitro release study

In vitro release was performed by dialysis membrane method. A formulation quantity equivalent to 5 mg prednisolone was placed in a pre-soaked dialysis bag and immersed in 100 mL release medium at 37 ± 0.5°C under 100 rpm shaking. The medium sequence was 0.1 N HCl pH 1.2 for 2 h, phosphate buffer pH 6.8 for 4 h and phosphate buffer pH 7.4 up to 24 h. At each sampling point, 2 mL medium was withdrawn and replaced with fresh medium.

2.9 Release kinetic modelling

Release data for the optimized formulation were fitted to zero-order, first-order, Higuchi, Korsmeyer-Peppas and Hixson-Crowell models. The best descriptor was selected using the coefficient of determination (R2) together with mechanistic plausibility [25-28].

2.10 Mucin binding, hemocompatibility, Caco-2 viability and stability

Mucin binding was evaluated by mixing nanoparticle dispersion (1 mg/mL) with mucin solution (1 mg/mL) in phosphate buffer pH 7.4 at 1:1 ratio and incubating at 37°C for 5-60 min. Free mucin in the supernatant was estimated colorimetrically after centrifugation. Hemocompatibility was evaluated by incubating formulation dispersions of 50-400 ug/mL with erythrocyte suspension at 37°C for 1 h, using normal saline as negative control and distilled water as positive hemolysis control. Caco-2 cells were exposed to 12.5-400 ug/mL formulation for 24 h and assessed by MTT assay. Optimized lyophilized nanoparticles were stored at 4 ± 2°C and 25 ± 2°C/60 ± 5% RH for six months, and particle size, PDI, zeta potential, drug content and entrapment efficiency were periodically evaluated.

2.11 Statistical analysis and figure preparation

Experiments were performed in triplicate unless otherwise stated, and results are presented as mean ± standard deviation. Design data were interpreted by polynomial regression and response surface analysis. The grayscale figures were prepared without grid lines using pattern-filled bars or line markers, and SD/error bars were included. For the Box-Behnken response plots, the original design table did not provide run-wise replicate SD values for every run; therefore, pooled center-point variability from repeated center runs was used as the error-bar estimate for visualization. The raw replicate SD values should be substituted before final journal submission if available.

III. RESULTS

3.1 Analytical linearity and formulation appearance

The prednisolone analytical method was linear over 5-100 ug/mL with regression equation y = 0.0118x + 0.0064 and R2 = 0.9987. The optimized lyophilized coated nanoparticles appeared as an off-white free-flowing powder. On redispersion in distilled water, the optimized batch formed a uniform milky dispersion without visible aggregates after mild shaking and short sonication.

3.2 Design responses and formulation-variable effects

Across the 17 design batches, particle size ranged from 190.82 to 252.66 nm, PDI from 0.172 to 0.244, zeta potential from -19.40 to -27.51 mV, entrapment efficiency from 63.99 to 78.97%, yield from 65.76 to 76.95% and 24 h release from 64.33 to 72.46%. Increasing the PLGA amount generally increased particle size and drug entrapment because of higher polymeric solid content and greater drug-retaining matrix volume. PVA improved dispersion stabilization, although high stabilizer concentration could alter viscosity and interfacial behavior. Eudragit S100 increased the negative surface character and contributed to pH-dependent protection.

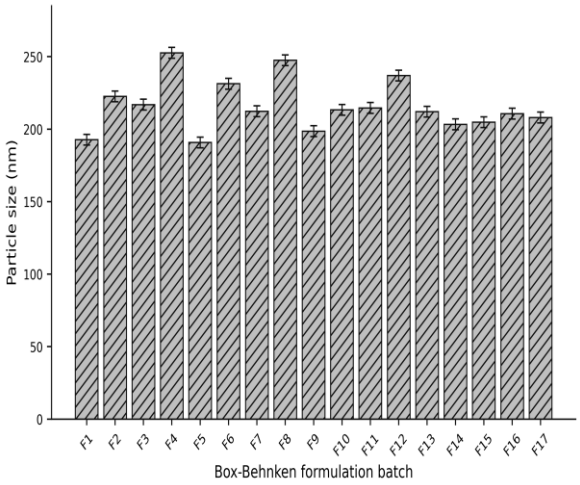

Figure 2. Particle size response of Box-Behnken design batches. Bars are grayscale/patterned with no grid lines; error bars show pooled center-point SD used for visualization where run-wise SD values were unavailable.

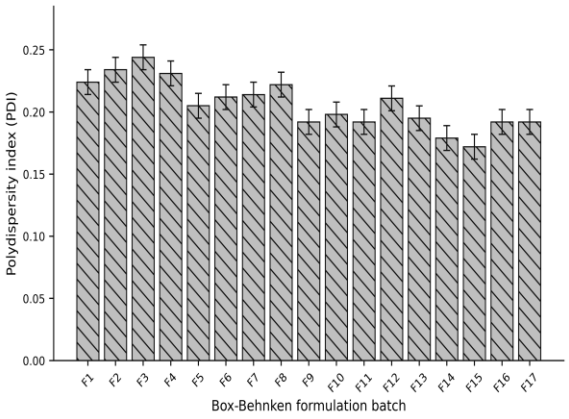

Figure 3. PDI response of Box-Behnken design batches. Lower PDI values indicate a narrower size distribution. Error bars represent pooled center-point SD.

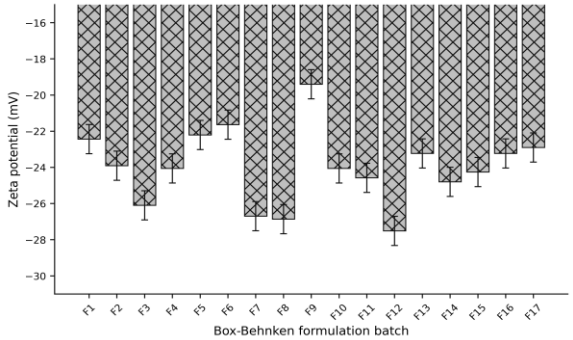

Figure 4. Zeta-potential response of Box-Behnken design batches. Greater negative magnitude reflects stronger surface charge contribution, largely associated with Eudragit S100 coating. Error bars represent pooled center-point SD.

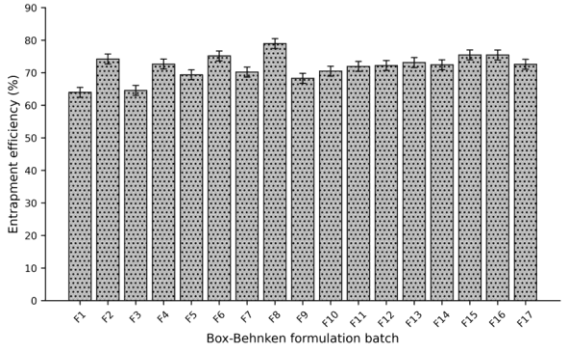

Figure 5. Entrapment-efficiency response of Box-Behnken design batches. Error bars represent pooled center-point SD.

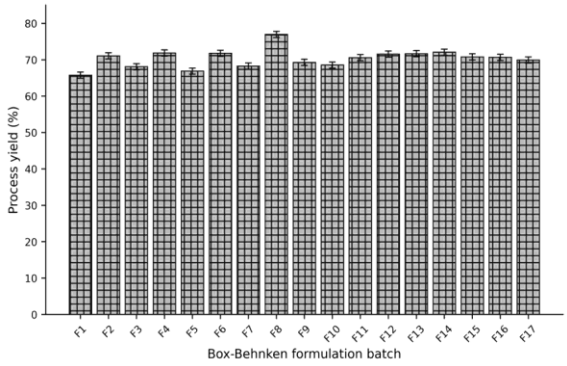

Figure 6. Process-yield response of Box-Behnken design batches. Error bars represent pooled center-point SD.

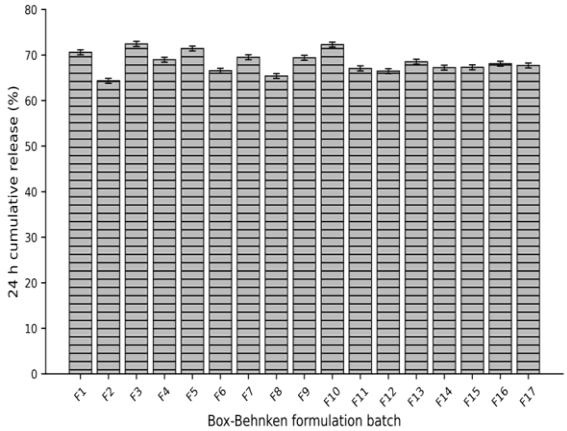

Figure 7. Twenty-four-hour cumulative release response of Box-Behnken design batches. Error bars represent pooled center-point SD.

3.3 Optimized formulation and confirmatory characterization

The optimized formulation contained PLGA 120 mg, PVA 0.6% w/v and Eudragit S100 75 mg. This composition was selected because it provided a practical compromise between nanoscale size, acceptable PDI, negative zeta potential, high entrapment, reasonable yield and sustained 24 h release. The optimized coated formulation showed particle size of 214.6 ± 6.8 nm, PDI of 0.214 ± 0.018, zeta potential of -31.8 ± 1.6 mV, entrapment efficiency of 82.4 ± 2.1%, drug content of 96.8 ± 2.7% and 24 h cumulative release of 76.9 ± 3.1% (Table 2).

Table 2. Summary of optimized Eudragit S100-coated prednisolone-loaded PLGA nanoparticles.

Parameter	Observed value	Target/interpretation
Composition	PLGA 120 mg; PVA 0.6% w/v; Eudragit S100 75 mg	Balanced optimized batch

Parameter	Observed value	Target/interpretation
Particle size	214.6 ± 6.8 nm	Nanoscale dispersion appropriate for mucosal interaction
PDI	0.214 ± 0.018	Acceptable narrow distribution
Zeta potential	-31.8 ± 1.6 mV	Negative surface charge after coating
Drug content	96.8 ± 2.7%	Uniform drug incorporation
Entrapment efficiency	82.4 ± 2.1%	Efficient loading in polymeric matrix
24 h cumulative release	76.9 ± 3.1%	Sustained release under sequential pH conditions

3.4 pH-sequential release behavior

The free drug showed rapid release, reaching 62.10 ± 2.1% at 2 h and approximately complete release by 24 h. Uncoated prednisolone nanoparticles slowed the release compared with free prednisolone, whereas Eudragit S100-coated nanoparticles restricted release to 8.70 ± 3.1% during the first 2 h in acidic medium. After transition to pH 6.8 and 7.4, the coated system exhibited progressive release, reaching 76.90 ± 3.1% at 24 h (Table 3 and Figure 8). This profile supports the functional role of the pH-responsive coating in reducing premature acidic release.

Table 3. pH-sequential release profile of free prednisolone, uncoated nanoparticles and Eudragit S100-coated nanoparticles.

Time (h)	Free drug (%)	Uncoated PRD-NP (%)	Eudragit-coated PRD-NP (%)
0	0.00 ± 2.1	0.00 ± 2.5	0.00 ± 3.1
1	38.40 ± 2.1	18.20 ± 2.5	4.80 ± 3.1
2	62.10 ± 2.1	31.60 ± 2.5	8.70 ± 3.1
4	78.60 ± 2.1	45.30 ± 2.5	14.60 ± 3.1
6	88.20 ± 2.1	55.70 ± 2.5	21.20 ± 3.1
8	94.30 ± 2.1	63.80 ± 2.5	30.80 ± 3.1
12	98.10 ± 2.1	74.50 ± 2.5	47.50 ± 3.1
18	99.00 ± 2.1	83.90 ± 2.5	62.80 ± 3.1
24	100.20 ± 2.1	91.40 ± 2.5	76.90 ± 3.1

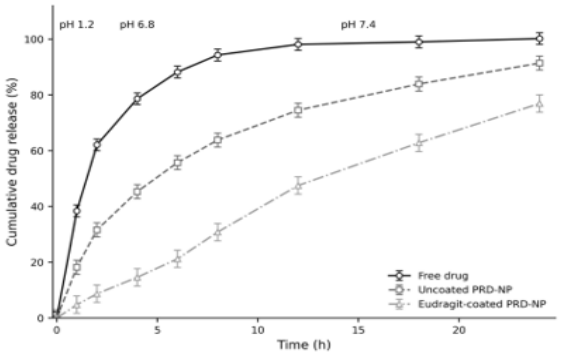

Figure 8. pH-sequential in vitro release profile of free prednisolone, uncoated PRD-NP and Eudragit S100-coated PRD-NP (mean ± SD, n = 3).

3.5 Mucin binding and preliminary in vitro compatibility

The optimized coated nanoparticles showed time-dependent interaction with mucin, increasing from 18.0 ± 1.2% at 5 min to 79.4 ± 3.8% at 60 min (Figure 9). This behavior suggests favorable interaction with mucus components, which may be relevant for residence at inflamed colonic mucosa. Hemolysis remained below 5% up to 400 ug/mL, indicating acceptable preliminary blood compatibility under the tested conditions. Caco-2 cell viability remained above 75% up to 200 ug/mL and was 63.8 ± 4.2% at 400 ug/mL, indicating concentration-dependent but reasonable compatibility for further preclinical evaluation (Figure 10).

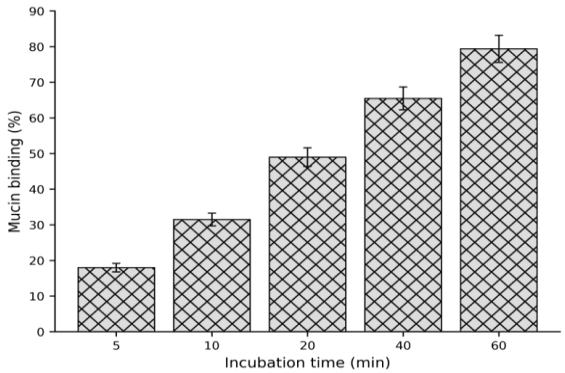

Figure 9. Time-dependent mucin binding of optimized coated prednisolone nanoparticles (mean ± SD, n = 3).

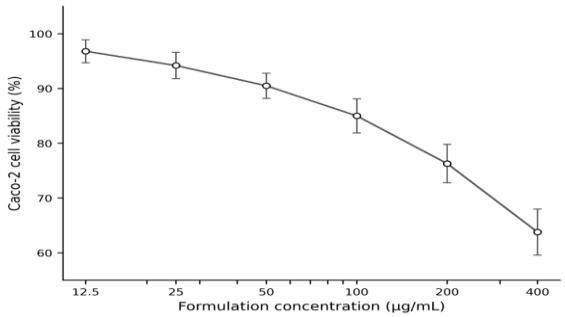

Figure 10. Caco-2 cell viability after exposure to optimized coated nanoparticles (mean ± SD, n = 3).

3.6 Stability evaluation

During six-month storage, particle size increased moderately from 214.6 ± 6.8 nm to 231.5 ± 8.9 nm, while entrapment efficiency decreased from 82.4 ± 2.1% to 77.8 ± 2.6%. No cake collapses or severe aggregation was observed. The moderate change in particle size and entrapment suggests that the lyophilized coated nanoparticles retained acceptable preliminary stability under the selected storage conditions (Figures 11 and 12).

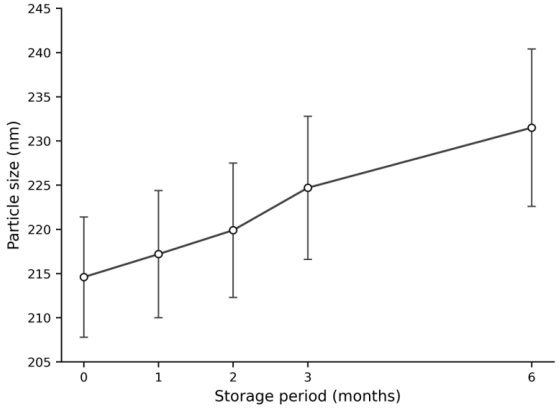

Figure 11. Particle-size trend of optimized coated nanoparticles during six-month storage (mean ± SD).

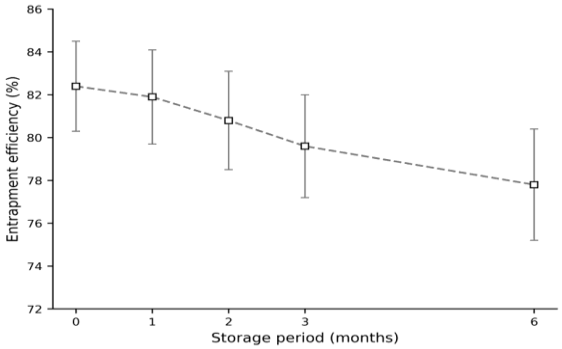

Figure 12. Entrapment-efficiency trend of optimized coated nanoparticles during six-month storage (mean ± SD).

3.7 Release kinetic modelling

The optimized coated formulation showed the highest coefficient of determination with the Higuchi model (R2 = 0.982), followed by the Korsmeyer-Peppas model (R2 = 0.975; n = 0.46). Zero-order, first-order and Hixson-Crowell fits were lower. These results indicate diffusion-dominant release with possible contribution of polymer relaxation and limited matrix erosion (Table 4 and Figure 13).

Table 4. Release kinetic model fitting for optimized coated prednisolone nanoparticles.

Model	Equation form	R2	Interpretation
Zero-order	Qt = Q0 + K0t	0.914	Not primary release model
First-order	log Q = log Q0 - Kt/2.303	0.887	Concentration dependence limited
Higuchi	Q = KH t1/2	0.982	Diffusion dominant
Korsmeyer-Peppas	Mt/M∞ = Ktn	0.975; n = 0.46	Fickian/anomalous diffusion
Hixson-Crowell	Q01/3 - Qt1/3 = KHct	0.931	Minor matrix erosion contribution

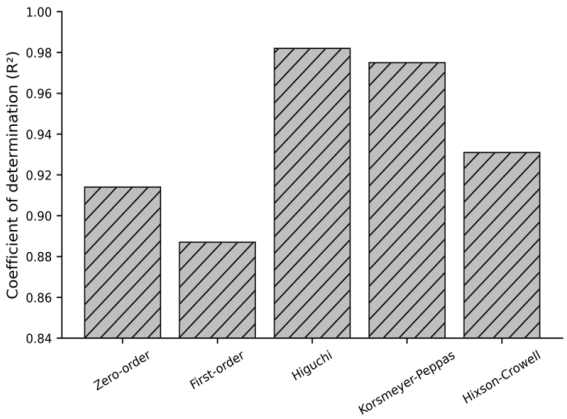

Figure 13. Comparative release-kinetic model fit for optimized coated prednisolone nanoparticles. SD is not applicable to R2 model-fit values.

IV. DISCUSSION

The study demonstrates that an enteric-coated biodegradable nanoparticle system can be rationally optimized for colon-targeted prednisolone delivery. The PLGA core provided a drug-retaining matrix, PVA stabilized the nanosuspension during solvent displacement and Eudragit S100 supplied pH-responsive protection against acidic release. The multi-response optimization strategy was essential because the same variable could improve one attribute while compromising another.

Particle size across the design remained within the nanoscale range, supporting successful solvent-displacement formation. Increasing polymer amount

generally increased size because the organic phase contained more polymeric solids available for precipitation. At the same time, higher polymer content improved drug retention and entrapment. This balance is important because excessive enlargement may reduce mucus interaction and redispersibility, while low polymer amount may reduce drug loading.

The pH-sequential release data are central to the colon-targeting rationale. Free prednisolone released rapidly, which would be undesirable for oral colon delivery because early liberation may increase upper gastrointestinal absorption and systemic exposure. Uncoated PLGA nanoparticles slowed release but did not provide sufficient acidic protection. Eudragit S100 coating markedly restricted release at pH 1.2 and allowed progressive release at higher pH, aligning with the intended delayed-release behavior.

Mucin binding suggested a potentially useful interaction with mucus components. For ulcerative colitis, prolonged residence near inflamed mucosa may improve local drug availability. Nevertheless, mucin binding alone does not confirm in vivo colonic retention because mucus turnover, disease severity, microbiota, transit time and motility can influence residence. The hemocompatibility and Caco-2 findings should also be interpreted as preliminary screening data rather than proof of clinical safety.

The kinetic modelling supported diffusion-dominant release with a contribution from polymer relaxation. Higuchi and Korsmeyer-Peppas models provided the best fit, indicating that drug diffusion through the polymeric matrix and coating hydration/dissolution likely contributed to the release process. The six-month stability data suggested acceptable preliminary storage behavior, although accelerated stability, moisture sensitivity, redispersion robustness and batch-to-batch reproducibility remain necessary for later development.

A limitation of the current dataset is that individual run-wise replicate SD values were not available for every Box-Behnken response. For the response graphs, pooled center-point SD was therefore used to show experimental variability visually. This is acceptable for an internal manuscript draft, but raw triplicate data should be used for final Q1 journal submission. Additional limitations include the absence of ex vivo colonic adhesion/permeation, animal colitis efficacy, pharmacokinetic distribution and long-term toxicity studies.

V. CONCLUSION

Eudragit S100-coated PLGA nanoparticles were successfully developed and optimized for colon-targeted prednisolone delivery. The optimized formulation showed nanoscale size, acceptable PDI, negative zeta potential, high drug entrapment, restricted acidic release and sustained release under simulated intestinal/colonic pH conditions. The release mechanism was diffusion-dominant, and preliminary mucin-binding, hemocompatibility, Caco-2 viability and stability findings supported further development. The formulation should next be evaluated using ex vivo colonic tissue, inflamed-mucus interaction models, pharmacokinetic studies and animal models of ulcerative colitis.

DECLARATIONS

Author contributions

Conceptualization: [Name]; methodology: [Name]; investigation: [Name]; data curation: [Name]; writing-original draft: [Name]; writing-review and editing: [Name]; supervision: [Name].

Funding

No specific external funding is declared. Replace this statement if funding was received.

Ethics statement

The hemocompatibility experiment involved blood-based testing. Institutional ethics approval, consent details and donor-related information should be inserted before journal submission if human blood was used.

Conflict of interest

The authors declare no competing interests. Replace this statement if any conflict exists.

Data availability

The processed data used for the tables and figures are included in the manuscript and supplementary table. Raw replicate data should be made available by the authors upon reasonable request.

REFERENCES

[1] G. J. Bennett and Y. K. Xie, “A peripheral mononeuropathy in rat that produces disorders of pain sensation like those seen in man,” *Pain*, vol. 33, no. 1, pp. 87–107, 1988.

[2] Z. Seltzer, R. Dubner, and Y. Shir, "A novel behavioral model of neuropathic pain disorders produced in rats by partial sciatic nerve injury," *Pain*, vol. 43, no. 2, pp. 205–218, 1990.

[3] S. H. Kim and J. M. Chung, "An experimental model for peripheral neuropathy produced by segmental spinal nerve ligation in the rat," *Pain*, vol. 50, no. 3, pp. 355–363, 1992.

[4] C. J. Woolf and R. J. Mannion, "Neuropathic pain: aetiology, symptoms, mechanisms and management," *Lancet*, vol. 353, no. 9168, pp. 1959–1964, 1999.

[5] J. Scholz and C. J. Woolf, "Can we conquer pain?" *Nature Neuroscience*, vol. 5, Suppl., pp. 1062–1067, 2002.

[6] T. S. Jensen and R. Baron, "Translation of symptoms and signs into mechanisms in neuropathic pain," *Pain*, vol. 102, nos. 1–2, pp. 1–8, 2003.

[7] R. H. Dworkin, M. Backonja, M. C. Rowbotham, R. R. Allen, C. R. Argoff, G. J. Bennett, *et al.*, "Advances in neuropathic pain diagnosis and treatment," *Archives of Neurology*, vol. 60, no. 11, pp. 1524–1534, 2003.

[8] C. J. Woolf, "Pain: moving from symptom control toward mechanism-specific pharmacologic management," *Annals of Internal Medicine*, vol. 140, no. 6, pp. 441–451, 2004.

[9] M. Costigan, J. Scholz, and C. J. Woolf, "Neuropathic pain: a maladaptive response of the nervous system to damage," *Annual Review of Neuroscience*, vol. 32, pp. 1–32, 2009.

[10] L. Colloca, T. Ludman, D. Bouhassira, R. Baron, A. H. Dickenson, D. Yarnitsky, *et al.*, "Neuropathic pain," *Nature Reviews Disease Primers*, vol. 3, Art. no. 17002, 2017.

[11] R. Baron, A. Binder, and G. Wasner, "Neuropathic pain: diagnosis, pathophysiological mechanisms and treatment," *Lancet Neurology*, vol. 9, no. 8, pp. 807–819, 2010.

[12] N. B. Finnerup, R. Kuner, and T. S. Jensen, "Neuropathic pain: from mechanisms to treatment," *Physiological Reviews*, vol. 101, no. 1, pp. 259–301, 2021.

[13] Muthuraman, N. Singh, and A. S. Jaggi, "Protective effect of standardized extract of *Ocimum sanctum* against neuropathic pain in rats," *Journal of Ethnopharmacology*, vol. 120, no. 1, pp. 56–62, 2008.

[14] U. M. Aswar, A. D. Kandhare, V. Mohan, and P. A. Thakurdesai, "Neuroprotective effect of hesperidin in neuropathic pain," *Biomedicine & Pharmacotherapy*, vol. 97, pp. 1347–1358, 2018.

[15] P. J. Austin, C. F. Kim, C. J. Perera, and G. Moalem-Taylor, "Regulatory T cells attenuate neuropathic pain following peripheral nerve injury," *Pain*, vol. 153, no. 9, pp. 1916–1931, 2012.

[16] T. Várkonyi and P. Kempler, "Diabetic neuropathy: new strategies for treatment," *Diabetes, Obesity and Metabolism*, vol. 10, no. 2, pp. 99–108, 2008.

[17] B. Halliwell and J. M. C. Gutteridge, *Free Radicals in Biology and Medicine*, 5th ed. Oxford, U.K.: Oxford Univ. Press, 2015.

[18] O. H. Lowry, N. J. Rosebrough, A. L. Farr, and R. J. Randall, "Protein measurement with the Folin phenol reagent," *Journal of Biological Chemistry*, vol. 193, no. 1, pp. 265–275, 1951.

Supplementary material

Supplementary Table S1 provides the complete box-Behnken design matrix and measured responses used for optimization and graph preparation.

Supplementary Table S1. Complete Box-Behnken design response matrix.

Run	PLGA (mg)	PVA (% w/v)	Eudragit S100 (mg)	Size (nm)	PDI	Zeta (mV)	EE (%)	Yield (%)	Release 24 h (%)
1	80	0.3	75	192.71	0.224	-22.44	63.99	65.76	70.59
2	160	0.3	75	222.59	0.234	-23.91	74.23	71.06	64.33
3	80	0.9	75	216.92	0.244	-26.10	64.59	68.09	72.46
4	160	0.9	75	252.66	0.231	-24.06	72.69	71.86	68.98

Run	PLGA (mg)	PVA (% w/v)	Eudragit S100 (mg)	Size (nm)	PDI	Zeta (mV)	EE (%)	Yield (%)	Release 24 h (%)
5	80	0.6	50	190.82	0.205	-22.21	69.39	66.88	71.42
6	160	0.6	50	231.34	0.212	-21.64	75.18	71.77	66.54
7	80	0.6	100	212.33	0.214	-26.70	70.22	68.25	69.51
8	160	0.6	100	247.52	0.222	-26.86	78.97	76.95	65.40
9	120	0.3	50	198.59	0.192	-19.40	68.30	69.28	69.42
10	120	0.9	50	213.31	0.198	-24.06	70.50	68.54	72.31
11	120	0.3	100	214.64	0.192	-24.58	71.95	70.57	67.07
12	120	0.9	100	236.94	0.211	-27.51	72.23	71.56	66.49
13	120	0.6	75	212.06	0.195	-23.23	73.14	71.67	68.54
14	120	0.6	75	203.32	0.179	-24.80	72.47	72.07	67.24
15	120	0.6	75	204.81	0.172	-24.26	75.49	70.80	67.32
16	120	0.6	75	210.69	0.192	-23.23	75.46	70.66	68.11
17	120	0.6	75	208.02	0.192	-22.90	72.60	69.93	67.70

Note: For response-graph error bars, pooled center-point variability from runs 13-17 was used where run-wise SD values were not available. Raw triplicate SD values should be inserted for formal submission if available.